



On the End-to-End Latency of Cellular-Connected UAV Communications

Zhu, Hong; Rodríguez-Piñeiro, José ; Huang, Zeyu ; Domnguez-Bolano, Tomas; Cai, Xuesong; Yin, Xuefeng; Lee, Juyul; Matolak, David

Published in:

2021 15th European Conference on Antennas and Propagation (EuCAP)

DOI (link to publication from Publisher):

[10.23919/EuCAP51087.2021.9411072](https://doi.org/10.23919/EuCAP51087.2021.9411072)

Publication date:

2021

Document Version

Accepted author manuscript, peer reviewed version

[Link to publication from Aalborg University](#)

Citation for published version (APA):

Zhu, H., Rodríguez-Piñeiro, J., Huang, Z., Domnguez-Bolano, T., Cai, X., Yin, X., Lee, J., & Matolak, D. (2021). On the End-to-End Latency of Cellular-Connected UAV Communications. In *2021 15th European Conference on Antennas and Propagation (EuCAP)* [9411072] IEEE. <https://doi.org/10.23919/EuCAP51087.2021.9411072>

General rights

Copyright and moral rights for the publications made accessible in the public portal are retained by the authors and/or other copyright owners and it is a condition of accessing publications that users recognise and abide by the legal requirements associated with these rights.

- Users may download and print one copy of any publication from the public portal for the purpose of private study or research.
- You may not further distribute the material or use it for any profit-making activity or commercial gain
- You may freely distribute the URL identifying the publication in the public portal -

Take down policy

If you believe that this document breaches copyright please contact us at vbn@aub.aau.dk providing details, and we will remove access to the work immediately and investigate your claim.

On the End-to-End Latency of Cellular-Connected UAV Communications

Hong Zhu*, José Rodríguez-Piñeiro*, Zeyu Huang^{||}, Tomás Domínguez-Bolaño[†], Xuesong Cai[¶],
Xuefeng Yin*, Juyul Lee[‡], David Matolak[§]

*College of Electronics and Information Engineering, Tongji University, Shanghai, China,
{zhuhong0120,j.rpineiro,yinxuefeng}@tongji.edu.cn

^{||}CD-Lab for Dependable Wireless Connectivity, Institute of Telecommunications, TU Wien, zeyu.huang@tuwien.ac.at

[†]Department of Computer Engineering, University of A Coruña, A Coruña, Spain, tomas.bolano@udc.es

[¶]Department of Electronic Systems, Aalborg University, Aalborg, 9220, Denmark, xuc@es.aau.dk

[‡]Telecomm. Media Research Lab, Electronics & Telecomm. Research Institute (ETRI), Daejeon, Korea, juyul@etri.re.kr

[§]Department of Electrical Engineering, University of South Carolina, Columbia, SC, USA, matolak@cec.sc.edu

Abstract—Unmanned Aerial Vehicles (UAVs) have been widely used in military and civilian fields in the recent years. In order to give support to the vast amount of added value services, UAV communications have become a hot spot for the fifth generation (5G) and have a very broad development prospect. In this paper, based on the channel modeling results obtained by actual measurements, we evaluate the end-to-end delay of Long Term Evolution (LTE) for air-to-ground (A2G) communications in suburban environments. The results show that, in order to satisfy the reliability and latency requirements of the critical communications, the base stations (BSs) deployment and the flight routes need to be carefully considered since small increments on the flight distance can have great influence on the packet success rate and the end-to-end delay. The obtained results are of great importance to evaluate if current LTE deployments can support critical communications for cellular-connected UAVs.

Index Terms—Unmanned Aerial Vehicle (UAV), air-to-ground communications, end-to-end delay, Long Term Evolution (LTE)

I. INTRODUCTION

The number of Unmanned Aerial Vehicles (UAVs) has experienced a dramatic increase in recent years due to their steadily decreasing cost and the fast-growing demand both in military and civilian fields. UAVs can be used for emergency search and rescue operations, traffic real-time monitoring, communications relaying applications, etc. [1], [2]. It is noteworthy that these applications for UAVs mostly rely on UAV communications, especially air-to-ground (A2G) communications, which are usually defined as those using a link between the UAV and a terrestrial base station (BS). A2G communications can serve many practical purposes, such as to transmit data or video from the UAV to the BS, or to receive control signals from a terrestrial commander. Therefore, it is crucial to investigate whether the requirements of availability, Quality of Service (QoS), latency and throughput for different applications can be fulfilled.

Efforts have been taken in the literature to characterize the A2G propagation channel, which can be categorized into measurement-based ones and simulation-based ones, respectively. Based on measurement campaigns, channel characteristics including path loss, shadow fading, Doppler frequency

spread, delay spread or K-Factor for UAV communications in different scenarios have been investigated [3]–[9]. By means of simulations, the performance of communications can be studied based on the (possibly measurement-based) established channel models, such as in our previous work, [10], which is solely based on the study of the throughput. Although in that work we have illustrated that when the signal to noise ratio (SNR) is greater than 0 dB, the channel equalization techniques can compensate most of the large and small-scale effects, we did not consider the end-to-end latency of communications (i.e., the time taken for a data packet for being received successfully after being transmitted). As a matter of fact, there has been little discussion about end-to-end delay of A2G communications for small low-height UAVs in the related literature. It is important to highlight that the end-to-end delay is especially crucial for the so-called critical communications. Since these kinds of communications transmit safety- and control-related messages, the 3rd Generation Partnership Project (3GPP) have imposed high reliability constraints for them, and hence low tolerance to errors and low delay [11]. Therefore, the performance of A2G communications for low-height UAVs in terms of end-to-end delay needs to be assessed based on realistic channel models.

In this work, we consider the evaluation of the performance of A2G communications not only focused on the throughput, but also on the end-to-end delay, which implies considering both the forward link (transmissions from the BS to the UAV) and the feedback one (transmissions from the UAV to the BS). Our results are obtained by means of simulations but using the channel extracted from our previous measurement campaign described in [4], carried out in a suburban scenario in which a single UAV flies at a constant height while communicating to a terrestrial BS. The data packet retransmission mechanisms of Long Term Evolution (LTE) are considered and the results show the influence of the distance between the BS and the UAV both in end-to-end delay as well as in the rate of packets lost, which also influence the throughput and the reliability of the communications. The results, presented in a comprehensive way, show that the flight distance should

be carefully considered if critical communications, such as control commands, will be transmitted by an A2G link.

II. RETRANSMISSION MECHANISMS IN LTE

The LTE retransmission mechanisms are investigated to show the tendency of end-to-end delay with respect to flight distance. According to the LTE standard, a cyclic redundancy check (CRC) is used when transmitting data [12]. The receiver is in charge of checking the correctness of the CRC received along with each data packet and (possibly) request a retransmission if errors are detected. In order to do so, a Hybrid Automatic Repeat reQuest (HARQ) technique, which combines both Automatic Repeat reQuest (ARQ) with Forward Error Correction (FEC), is considered in LTE. When the receiver gets a new packet with errors (hence, wrong CRC), it firstly tries to correct it by means of a FEC technique. If there are no remaining errors in the packet, the HARQ indicator will be set to 0 (equivalently, a positive acknowledgement (ACK) is returned to the transmitter). However, if the errors cannot be corrected completely, the HARQ indicator will set to 1 (negative acknowledgement (NACK) is sent back to the transmitter) and the transmitter will retransmit that packet. After getting the data again, the receiver combines the newly received data with that of previous erroneous attempts and tries to perform the correction again [13] [14, Section 9.3.4].

We define a HARQ process as the logical entity in charge of transmitting a data packet, including tracking of the eventual retransmissions. As defined in LTE, there will be up to 8 HARQ processes generated simultaneously [14, Section 10.3.2.5], which means that the retransmissions of 8 packets are handled in parallel, although of course a single packet is retransmitted at a time. It should be noticed that the HARQ processes are allowed to perform transmissions not necessarily in a sequential way, i.e., the order of transmissions of packets cannot be predicted in principle.

Some concepts regarding are described below to help the readers to better understand the results of our work:

- Number of transmissions for a packet: number of attempts required to transmit a packet.
- Packet transmitted successfully: when there are no remaining errors to be corrected for a received packet and the receiver replies with an ACK to the transmitter, we consider the packet as transmitted successfully.
- Lost packet: when the errors in a packet cannot be fully corrected and hence a retransmission occurs, the transmission times for that packet will be increased into one unit until it equals to 4. When the packet transmission times equals to 4 (i.e., there were four attempts of sending the packet) and there are still remaining errors, the packet will be dropped by LTE [14, Section 10.3.2.5]. The application layer [15] will be responsible of handling the lost packets.
- Packet end-to-end delay (also referred as end-to-end latency): time instant when a packet is received correctly (ACK is sent by receiver) minus the time instant when it is transmitted for the first time (transmission times equal

to 1). Note that additional delays can be introduced by higher levels of the communication system [15].

III. MEASUREMENT CAMPAIGN AND CHANNEL MODEL

A. Measurement environment and equipment

The measurement campaign described in [4] was considered for this study (in particular, one of the flights performed on it). The channel measurement campaign was carried in a suburban scenario at the Jiading Campus of Tongji University, China. Fig. 1a shows the measurement environment, consisting of buildings around 15 – 30 m high, roads, rivers, grassland and trees. A straight dotted line, joining the so-called “starting point” and “end point”, denotes the UAV flight route considered¹. The BS is aligned with the flight route and approximately 20 m away from the starting point, as represented in the figure². The UAV flies at a height of 60 m and at a speed of 5 m/s. The propagation conditions can be regarded as line-of-sight (LoS).

A custom-built A2G channel sounder, described into detail in [4], was used for the channel measurements. The transmitter is fixed on a lift at 15 meters high, working as the BS, whereas the receiver is installed on the UAV. Fig. 1b shows the details of the sounder, including the UAV and the BS. Both the UAV and the BS are equipped with Global Positioning System (GPS)-disciplined oscillators, identical quasi-omnidirectional antennas and a Universal Software Radio Peripheral (USRP) N-210 used to transmit (BS) and receive (UAV) signals. Besides, the BS part also has a power amplifier and a power source and the UAV part also has a small computer to collect the data from USRP and a router (used exclusively to control the small computer by a ground operator).

The central carrier frequency of the measurements is 2.5 GHz³ and the bandwidth 15.36 MHz, which are close to the actual values used for the LTE commercial services in the measurements area. In addition, an orthogonal frequency-division multiplexing (OFDM) signal following a frame structure similar to that of downlink LTE was considered as the sounding signal.

B. Acquired signals processing and extracted channel model

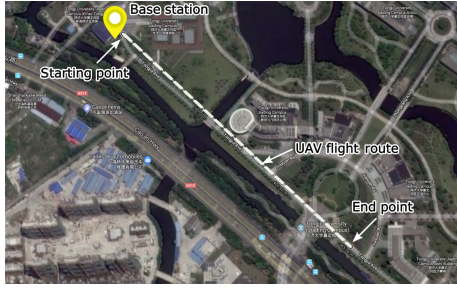
The so-called “GTEC 5G Simulator” [16], [17] was used to generate and process the signals⁴. The GTEC 5G Simulator not only can flexibly generate the transmit signals, but also implements all the necessary modules in order to process the acquired signals, such as channel estimation, interpolation and equalization algorithms, as well as time and frequency synchronization. The acquired OFDM frames were further

¹Coordinates of the starting point and end point (latitude, longitude): (31.287433°, 121.204179°) and (31.284102°, 121.208412°), respectively.

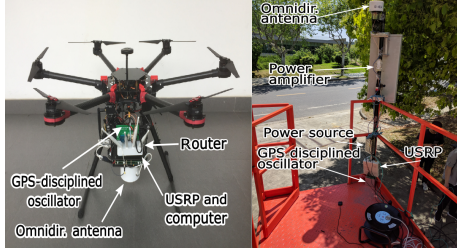
²Coordinates of the transmitter (latitude, longitude): (31.2873872°, 121.2040907°).

³Note that the wireless local area network (WLAN) connection used to control the small computer on the UAV from the ground causes no interference to the measurements since it works in the frequency band of 2.4 GHz.

⁴The source code of both the GTEC Testbed and the GTEC 5G Simulator is publicly available under the GPLv3 license at https://bitbucket.org/tomas_bolano/gtec_testbed_public.git.



(a) Measurement environment.



(b) Picture of the A2G channel sounder.

Fig. 1: Measurement sounder and environment.

processed by the space-alternating generalized expectation-maximization (SAGE) algorithm [18] integrated in the “GTEC 5G Simulator”, allowing to estimate the channel Multipath Components (MPCs). A *snapshot* is regarded as the set of MPCs obtained from the signal samples corresponding to an observation period, which approximately equals to 10 ms in our measurements. The channel impulse response for the m -th snapshot is

$$h_m(t, \tau) = \sum_{l=1}^L \alpha_{m,l} \delta(\tau - \tau_{m,l}) e^{j2\pi\nu_{m,l}t}. \quad (1)$$

In Eq. (1), t is the time variable, τ represents the delay, $\alpha_{m,l}$, $\tau_{m,l}$ and $\nu_{m,l}$ are respectively the complex amplitude, delay and Doppler frequency for the l -th path of m -th snapshot, $\delta(\cdot)$ denotes the impulse function (Dirac delta) and L is the number of MPCs per snapshot. In order to capture most of the received power, $L = 15$ paths are considered in our measurements according to the observations in [4]. Since $\alpha_{m,l}$, $\tau_{m,l}$ and $\nu_{m,l}$ are constant for each snapshot, only the term including the Doppler frequency in Eq. (1) changes within each observation period.

The captured channel snapshots are used to simulate the transmission of LTE signals in order to estimate the end-to-end packet delay, packet success rate and resulting throughput. The received i -th LTE subframe can be written in the time domain as:

$$y_i(t) = x_i(t) * h_m(t, \tau) + n(t). \quad (2)$$

In Eq. (2), $x_i(t)$ is the transmitted signal corresponding to the i -th LTE subframe in time domain, $*$ is the time-varying convolution operator, m is the number of snapshot corresponding to the i -th LTE subframe, and $n(t)$ is additive white Gaussian noise (AWGN).

The power of the AWGN for the simulations is adjusted to fit the SNR observed in the measurements. Fig. 2 shows a comparison between the simulated and the measured SNR versus the so-called horizontal distance, defined as the projection of the distance between the BS and the UAV on the ground. The measured SNR is represented by a dotted black curve whereas the simulated one by a solid blue curve. It can be seen that the measured values slightly deviate from the simulated values in some areas (e.g. between the horizontal distance 170 m and 200 m). However, the overall trend and values of the measured and simulated results are consistent.

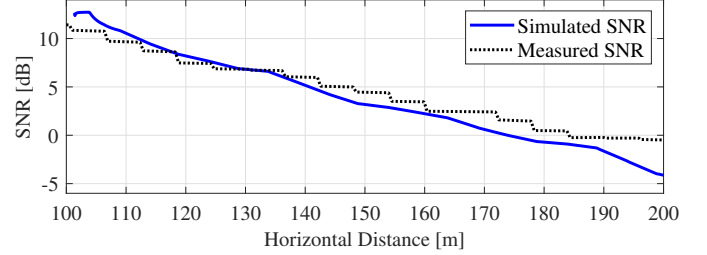


Fig. 2: Simulated SNR and measured SNR.

IV. SIMULATION RESULTS

A. Packet success rate and number of transmissions

The simulated SNR versus the horizontal distance between the UAV and the BS for the whole flight is shown in Fig. 3a. It is worth mentioning that the value of simulated SNR goes to 0 dB at about 175 m horizontal distance. Fig. 3b shows the number of transmissions per packet w.r.t. the horizontal distance between UAV and BS. It can be clearly seen that a single transmission attempt is required to ensure the successful transmission at the beginning of the flight. However, when the horizontal distance increases, more number of transmissions are needed to be combined in order to get a successfully transmitted packet. No more than 4 transmission attempts for one packet are considered, as explained in Section II. It can be seen that when the SNR is negative in dB, all the packets are transmitted 4 times.

The packet success rate w.r.t the horizontal distance obtained by using an average window of length 1 s is shown in Fig. 3c. It can be seen from Fig. 3c that the packet success rate is 100% at the beginning of the flight. It starts to decrease at about 166 m and at about 176 m the rate comes to 0% since there are no more packets received successfully. This shows that most of the packets that need four transmission attempts (see Fig. 3b) still fail after the fourth attempt and hence are discarded, as indicated in Section II. The rate of packet success rate descent is relatively high, which means that the performance of the communications reduces very fast in a short distance around the flight point in which the SNR decreases from 0 dB. According to the reliability requirements for UAV communications from the 3GPP [11], less than 0.1% packet error rate is allowed for critical communications. It can be seen that in our scenario this criterion is only fulfilled when the horizontal distance is lower than approximately 165 m.

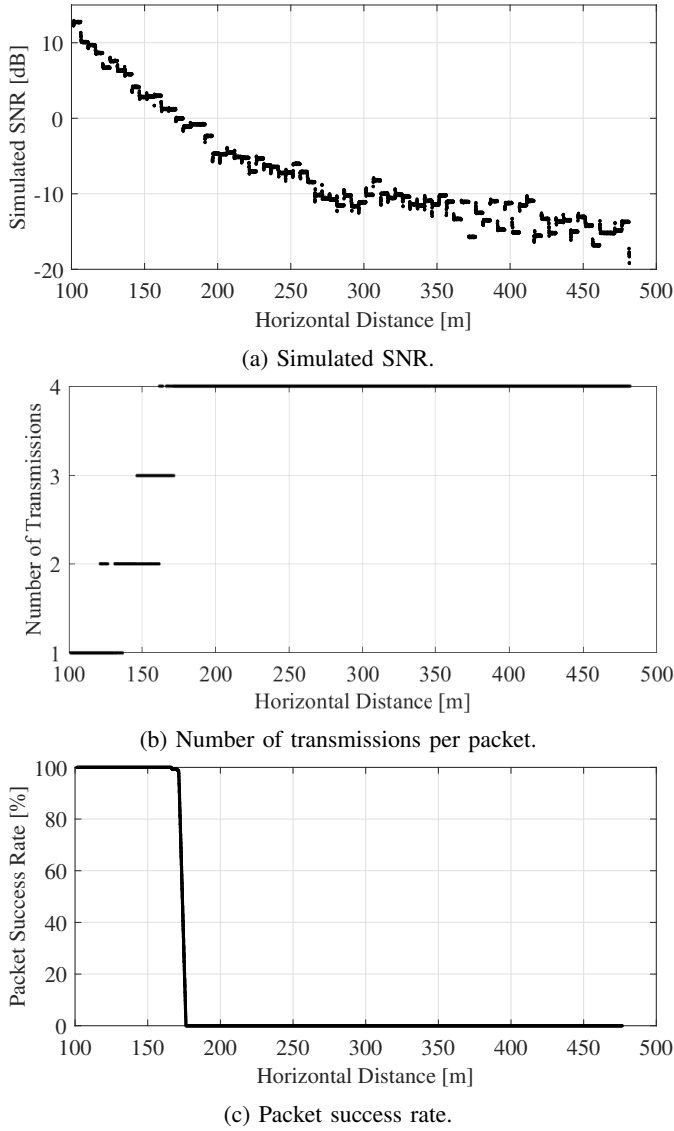


Fig. 3: Simulated SNR, number of transmissions per packet and packet success rate.

B. End-to-end delay

The end-to-end delay, defined in Section II, is crucial for critical communications. In other words, it is not only necessary to deliver the packets, but to deliver them on time. The fact that all the transmitted packets are lost for horizontal distances larger than 175 m does not mean that for shorter distances the performance is constant. This way, Fig. 4 shows the end-to-end delay w.r.t. the horizontal distance⁵. In Fig. 4, the X-axis is the horizontal distance between the UAV and the BS, and Y-axis is the delay per packet, which is represented by black dots. Along with the instantaneous values, a blue smoothed curve (obtained by moving average) is also provided to reveal the general trend of the delay. The minimum observed

⁵Note that only horizontal distance values lower than 180 m are considered, since no packets are received for longer distances.

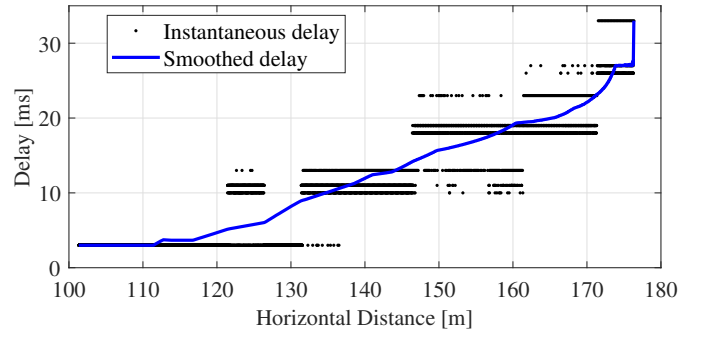


Fig. 4: End-to-end delay.

delay is 3 ms, which corresponds to the processing time of receiver [14, Section 10.3.2.5]. This value corresponds to the packets transmitted successfully in the first attempt, as shown in Section IV-A. However, when the flight distance increases and hence the SNR decreases, the delay becomes larger and takes one of several discrete values, which are determined by the order in which different HARQ processes retransmit the packets. Packets exceeding 4 transmission attempts are discarded, as indicated in Section II, which limits the maximum delay value. According to the constraints for UAV communications from the 3GPP [11], a latency lower than 50 ms is required for critical communications, which is fulfilled in our case for any packet that is not discarded due to exceeding the maximum number of transmission attempts. For our scenarios, this happens for all the horizontal distance values lower than 175 m. Note that we only consider the LTE delay in our simulations, and hence we do not include the delay of higher layers, e.g. the application layer.

C. Throughput

Fig. 5 shows the number of successfully received bits per packet w.r.t. the horizontal distance, which can be used to calculate the throughput. It can be observed that after 175 meters, no bits are received successfully and hence the instantaneous bits per packet values decrease to zero, which is consistent with the results shown in Section IV-A. It can be seen that there are three different values of bits received successfully per packet (0, 11448 and 12960). A 0 value means that the packet needs a retransmission, hence if no packets are failed, no zero values will appear. In other words, the first zero value will appear with the first packet needed to be retransmitted. For the packets that are transmitted successfully, two possible values for the bits per packet can be observed since different LTE subframes provide different payload capacity depending on the control signals that they include. The average throughput for the whole flight distance is 1.52 Mbps, whereas if only the distances below 175 m are considered, the average throughput becomes 7.72 Mbps. For the flight distances where no packets are retransmitted, which the average throughput is 12.85 Mbps. According to the constraints for UAV communications from the 3GPP [11], the data rate requirements for the downlink are

in the range of 60-100 Kbps, hence the throughput will not be a limiting factor when LTE is used, according to our results.

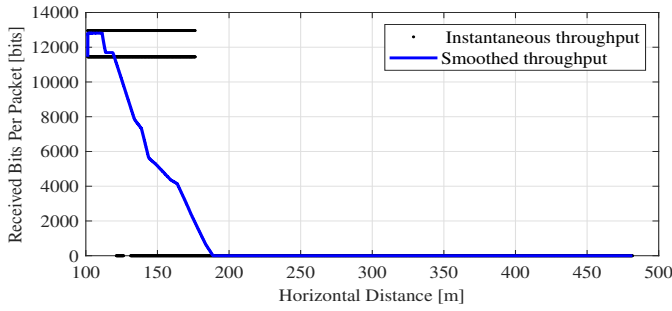


Fig. 5: Successfully received bits per packet.

V. CONCLUSIONS

In this paper, the performance of LTE for A2G communications was evaluated by simulations considering the channels captured in actual A2G measurements in suburban scenarios. Different from most of the previous works, we have characterized the performance not only by the throughput, but also by the end-to-end delay and the success rate of the transmitted packets. These results are especially relevant to determine whether LTE can support critical communications for A2G links with low-height small UAVs.

From the whole transmission process we can find that the performance of the A2G communication systems changes very quickly with the flight distance, severely impacting the packet success rate and end-to-end delay. When the flight distance is low, the packets are transmitted successfully at the first attempt, leading to the 100% packet success rate and the minimum possible end-to-end delay. For longer distances, higher number of transmissions per packet are needed to ensure the successful transmission, which also increases the end-to-end delay. It is noteworthy that when the SNR is about 0 dB, the performance of the channel drops very quickly, which is shown by the rapid decrease of the packet success rate. When the SNR is below 0 dB, there are no more packets transmitted successfully even if four attempts have been made and hence the packet success rate decreases to 0%. Hence, the instantaneous received bits per packet also come to zero. Finally, comparing the packet success rate results and end-to-end delay results with the reliability requirements and latency requirements of the critical communications proposed by 3GPP, respectively, we can find that it is essential to limit the maximum flight distance or to consider other kinds of antenna configurations depending on the intended applications to use. In general, the average throughput results are much higher than those required for critical communications. The obtained results show that the flight distance should be carefully planned when relying on cellular LTE network deployments for low-height UAV critical communications. Small increases in the flight distance can result in a sudden decrease of the performance and hence is not fulfilling the QoS and reliability requirements for this kind of communications.

ACKNOWLEDGMENT

This work was supported by the National Natural Science Foundation of China (61850410529, 61971313), the IITP grant funded by the Korean government (MSIT) (2017-0-00066), the Xunta de Galicia (ED431C 2020/15, ED431G2019/01), the Agencia Estatal de Investigación of Spain (RED2018-102668-T, PID2019-104958RB-C42) and ERDF funds of the EU (FEDER Galicia 2014-2020 & AEI/FEDER Programs, UE). The financial support by the Austrian Federal Ministry for Digital and Economic Affairs and the National Foundation for Research, Technology and Development is gratefully acknowledged.

REFERENCES

- [1] H. Shakhathreh, A. H. Sawalmeh, A. Al-Fuqaha, Z. Dou, E. Almaita, I. Khalil, N. S. Othman, A. Khreishah, and M. Guizani, "Unmanned aerial vehicles (UAVs): A survey on civil applications and key research challenges," *IEEE Access*, vol. 7, pp. 48 572–48 634, 2019.
- [2] Y. Zeng, R. Zhang, and T. J. Lim, "Wireless communications with unmanned aerial vehicles: opportunities and challenges," *IEEE Communications Magazine*, vol. 54, no. 5, pp. 36–42, 2016.
- [3] R. Amorim, H. Nguyen, P. Mogensen, I. Z. Kovcs, J. Wigard, and T. B. Srensen, "Radio channel modeling for UAV communication over cellular networks," *IEEE Wirel. Comm. Letters*, vol. 6, no. 4, pp. 514–517, 2017.
- [4] J. Rodríguez-Piñero, T. Domínguez-Bolaño, X. Cai, Z. Huang, and X. Yin, "Air-to-ground channel characterization for low-height UAVs in realistic network deployments," *IEEE Trans. Antennas Propag.*, vol. Early Access, 2020.
- [5] X. Cai, J. Rodríguez-Piñero, X. Yin, N. Wang, B. Ai, G. F. Pedersen, and A. P. Yuste, "An empirical air-to-ground channel model based on passive measurements in LTE," *IEEE Trans. Veh. Technol.*, vol. 68, no. 2, pp. 1140–1154, 2019.
- [6] X. Cai, N. Wang, J. Rodríguez-Piñero, X. Yin, A. Pérez-Yuste, W. Fan, G. Zhang, and G. F. Pedersen, "Low altitude air-to-ground channel characterization in LTE network," in *13th European Conference on Antennas and Propagation (EuCAP 2019)*, Krakow, Poland, 2019.
- [7] D. W. Matolak and R. Sun, "Air-ground channel characterization for unmanned aircraft systems-part I: Methods, measurements, and models for over-water settings," *IEEE Trans. Veh. Technol.*, vol. 66, no. 1, pp. 26–44, 2017.
- [8] —, "Air-ground channel characterization for unmanned aircraft systems-part III: The suburban and near-urban environments," *IEEE Trans. Veh. Technol.*, vol. 66, no. 8, pp. 6607–6618, 2017.
- [9] R. Sun and D. W. Matolak, "Air-ground channel characterization for unmanned aircraft systems part II: Hilly and mountainous settings," *IEEE Trans. Veh. Technol.*, vol. 66, no. 3, pp. 1913–1925, 2017.
- [10] Z. Huang, J. Rodríguez-Piñero, T. Domínguez-Bolaño, X. Yin, D. Matolak, and J. Lee, "Performance of 5G terrestrial network deployments for serving UAV communications," in *14th European Conf. on Antennas and Propagation (EuCAP 2020)*, Copenhagen, Denmark, 2020.
- [11] 3GPP, "Technical specification group radio access network: Study on enhanced LTE support for aerial vehicles," 3GPP, Tech. Rep. 3GPP TR 36.777 V15.0.0, December 2017.
- [12] —, "Multiplexing and channel coding," 3GPP, Tech. Rep. 3GPP TS 36.212 V8.0.0, 2007.
- [13] L. Yang and Z. Liao, "A hybrid automatic repeat request (HARQ) with turbo codes in OFDM system," in *2010 Intl. Conference on Computational Intelligence and Software Engineering*, 2010, pp. 1–4.
- [14] S. Sesia, I. Toufik, and M. Baker, *LTE-the UMTS long term evolution: from theory to practice*. John Wiley & Sons, 2011.
- [15] H. Zimmermann, "OSI reference model - the ISO model of architecture for open systems interconnection," *IEEE Transactions on Communications*, vol. 28, no. 4, pp. 425–432, 1980.
- [16] T. Domínguez-Bolaño, J. Rodríguez-Piñero, J. A. García-Naya, and L. Castedo, "The GTEC 5G link-level simulator," in *1st International Workshop on Link- and System Level Simulations (IWSLS2 2016)*, Vienna, Austria, July 2016.
- [17] "GTEC Testbed Project," https://bitbucket.org/tomas_bolano/gtec_testbed_public.git.
- [18] B. H. Fleury, M. Tschudin, R. Heddergott, D. Dahlhaus, and K. I. Pedersen, "Channel parameter estimation in mobile radio environments using the SAGE algorithm," *IEEE J. Sel. Areas Commun.*, vol. 17, no. 3, pp. 434–450, 1999.